AIAA JOURNAL
Vol. 34, No. 8, August 1996

Electrothermoelastic Behavior of Piezoelectric Coupled Cylinders

Mike Stam* and Greg Carman†
University of California, Los Angeles, Los Angeles, California 90024-1597

A coupled axisymmetric electrothermomechanical solution is presented for modeling the response of layered concentric cylinders exhibiting piezoelectric behavior. The governing equations for the problem are derived using conventional approaches incorporating electromechanical coupling terms and a unique higher order constitutive model that correctly reflects the strong dependence of the piezoelectric strain coefficients on temperature. This analytical approach suggests that stiffness values measured at constant electric displacement conditions are dependent on temperature due to depolarizing field influences. The layered concentric cylinder arrangement is used to model the quasistatic response of a piezoelectric linear motor currently proposed for space applications. Analytical/experimental results suggest that the nonlinear dependence of the piezoelectric coefficients with electric field can be extrapolated to lower temperatures using the proposed constitutive relation.

Introduction

BECAUSE of the exceptional promise that electromagnetothermomechanical (EMTM) materials offer when compared to conventional ones, EMTM materials are fast becoming a focal point for a variety of space-related research activities. For example, these materials offer remarkable potential in vibration suppression devices,[1] provide major enhancements for health monitoring systems,[2] and offer increased pointing accuracy in targeting and communication systems.[3] In fact, these material systems are being considered for controlling/positioning optical mirrors and articulating robotic arms in upcoming space missions.[4] However, conventional EMTM materials provide displacements on the order of microns and many of the space applications require displacements on the order of millimeters. To circumvent this limitation, researchers are evaluating EMTM-driven solid state motors providing the necessary displacements. Although these motors offer an attractive alternative to the monolithic material, a number of important questions must be answered prior to their implementation in space, such as temperature limitations, power requirements, and irradiation effects.

Solid state motors have been investigated by a number of scientists and engineers including the Niedermann et al.[5] version of a piezoelectric stick-slip mechanism and the Sakuta et al.[6] fine/coarse positioning piezoelectric motor. Another popular class of solid state motors providing large displacements are the piezoelectric ultrasonic motors. These motors use traveling surface acoustic waves to generate sizable motions.[7–9] In addition to piezoelectric motors, other EMTM systems are also being considered, such as shape memory materials for high-torque servomotors[10] and magnetostrictive materials for linear drivers.[11] Although all of these motors provide certain advantages and disadvantages, the class of piezoelectric linear motors (e.g., Refs. 12 and 13) represent one of the more promising solid state motor designs. These linear motors are well recognized for their long stroke (millimeters), precision pointing (nanometers), and absence of mechanical backlash. All of these characteristics make them an excellent candidate for positioning optical systems.

Conventional piezoelectric linear motors are arranged concentrically about a passive cylindrical shaft.[12] Therefore, the drive elements have cylindrically orthotropic material properties and can be analytically modeled with a concentric cylinders approach. Avery and Herakovich[14] presented an analytical solution for a passive cylindrical orthotropic material system to study the thermal induced stresses in an anisotropic fiber reinforced composite, and Cohen and Hyer[15] used a similar approach to model a layered composite material. More recent analytical developments related to EMTM material systems, include the Paine et al.[16] analysis of a cylindrical composite containing nitinol layers, Mitchell and Reddy's[17] finite element analysis for a piezoelectric cylindrical system using a constant field assumption, and the Adelman et al.[18] exact electroelastic solution for a piezoelectric cylinder subjected to a time varying electric field. In addition to these electromechanical models, researchers have analytically studied the electrothermomechanical behavior of piezoelectrics. Notable studies include Tzou and Ye[19] and Dunn.[20] However, current analytical modeling approaches do not incorporate the significant influence of temperature on the piezoelectric material properties.

The response of piezoelectrics at low temperatures has been experimentally studied by Jaffe and Berlincourt.[21] They demonstrated that the piezoelectric strain coefficients were strongly dependent on temperature, i.e., changed by over 50%. Therefore, this dependence must be included in analytical models evaluating the electrothermomechanical behavior of piezoelectric materials. Regarding constitutive modeling of this phenomenon, books by Parton and Kudryavtsev[22] and Ikeda[23] present analytical approaches that can be used to develop higher-order relations to account for the temperature influences. Recently, Wang et al.[24] used these analytical approaches along with experimental evidence to propose a constitutive model for piezoelectric materials, including the influence of temperature on the piezoelectric strain coefficients. In addition to thermal effects, Benedetto et al.[25] and Lorenz et al.[26] document several key features related to long-term exposures of ceramic ferroelectrics to radiation. Both of these experimental studies reach similar conclusions, that is, ferroelectrics do not degrade in exposures indicative of deep space missions. Therefore, irradiation influences are negligible for space applications. Power requirements and thermal issues, however, are a major concern.

We present a unique coupled analytical model to evaluate the electrothermomechanical response of a cylindrically arranged piezoelectric material system. The ceramic piezoelectric cylinder is poled radially with a spatially varying electric field induced in this direction. The constitutive relations are derived from a higher-order theory that incorporates the thermal/electrical/mechanical coupling between the coefficients. Therefore, the following analytical model is unique in the sense that it models the temperature dependence of the piezoelectric coupling coefficients. Parametric studies are presented for evaluating the quasistatic response of a specific linear motor constructed from a multilayered cylindrical system represented

Received Feb. 7, 1995; revision received June 14, 1995; accepted for publication Nov. 16, 1995.

*Research Assistant, Mechanical and Aerospace Engineering Department; currently Structural Design Engineer, Hughes Space and Communications Company, P.O. Box 92919, SC F25 C370, Los Angeles, CA 90002.

†Assistant Professor, Mechanical and Aerospace Engineering Department, 38-137 Engineering IV.

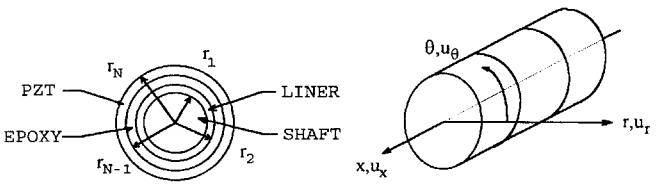

Fig. 1 Radii, coordinate axes, and displacements for an N-cylinder electrothermomechanical material system.

by an alumina shaft, silver liner, epoxy resin, and a piezoelectric ceramic (PZT-5h) arranged as shown in Fig. 1. Experimental data are presented to confirm the results obtained from the analytical model and demonstrate the strong dependence of these material systems on temperature. In addition to the electrothermomechanical solutions, we present an analytical development for power requirements patterned after the work by Moulson and Herbert[27] and compare these predictions with experimental data.

Electromechanical Elasticity Solution

In developing the electrothermoelastic analysis for a layered axisymmetric, anisotropic material system, the following assumptions are used. All materials are perfectly bonded together, are cylindrically orthotropic, exhibit linear elastic behavior, and are concentrically located. The material system is assumed to be axially long; therefore, end effects are ignored. A uniform temperature exists within all materials and only small strains are considered. The piezoelectric material is poled radially and a potential difference is applied in the radial direction. Applied loading and displacements are also axisymmetric. Subsequent equations are written in terms of cylindrical coordinates with axes ordered as θ, x, r, representing the circumferential, axial, and radial directions, respectively (see Fig. 1). The pertinent displacement variables are

$$\{u\}^T = [u_\theta, u_x, u_r] \tag{1}$$

and the stress and strain fields are

$$\{\sigma\}^T = [\sigma_\theta, \sigma_x, \sigma_r] \tag{2}$$

$$\{\varepsilon\}^T = [\varepsilon_\theta, \varepsilon_x, \varepsilon_r] \tag{3}$$

Because of the nature of the problem (i.e., symmetric boundary conditions, symmetric geometry, and symmetric material properties), shearing effects are not present. Because of this, strain values are depicted by a single subscript to avoid confusion with the dielectric permittivities that are presented with two subscripts. The electric displacement D_i and the electric field E_i variables are

$$\{D\}^T = [D_\theta, D_x, D_r] \qquad \{E\}^T = [E_\theta, E_x, E_r] \tag{4}$$

The electric field E_i is the negative gradient of the electric potential ϕ. Based on our axisymmetric and long cylinder assumption, ϕ is only a function of the radial direction and the only nonzero electric field is

$$E_r = -\frac{\partial \phi(r)}{\partial r} \tag{5}$$

The nonzero strain-displacement equations for a long axisymmetric cylinder are

$$\varepsilon_\theta = \frac{u_r(r)}{r}, \qquad \varepsilon_r = \frac{\partial u_r(r)}{\partial r}, \qquad \varepsilon_x = \text{const} \tag{6}$$

The relevant equation in the higher order constitutive relation for an electrothermomechanical material poled radially is[24]

$$\begin{Bmatrix} \sigma_\theta \\ \sigma_x \\ \sigma_r \end{Bmatrix} = \begin{bmatrix} C_{\theta\theta} & C_{\theta x} & C_{\theta r} \\ C_{x\theta} & C_{xx} & C_{xr} \\ C_{r\theta} & C_{rx} & C_{rr} \end{bmatrix} \begin{Bmatrix} \varepsilon_\theta - \alpha_\theta \Delta T \\ \varepsilon_x - \alpha_x \Delta T \\ \varepsilon_r - \alpha_r \Delta T \end{Bmatrix} - \begin{bmatrix} 0 & 0 & (e_{r\theta} + \bar{e}_{r\theta}\Delta T) \\ 0 & 0 & (e_{rx} + \bar{e}_{rx}\Delta T) \\ 0 & 0 & (e_{rr} + \bar{e}_{rr}\Delta T) \end{bmatrix} \begin{Bmatrix} 0 \\ 0 \\ E_r \end{Bmatrix} \tag{7}$$

where the stiffness terms $C_{\gamma\beta}$ are measured at constant temperature and constant electric field and α_i are the coefficients of thermal expansion (CTE) measured at constant electric field. The constitutive relation for the electric displacements is

$$\begin{bmatrix} D_\theta \\ D_x \\ D_r \end{bmatrix} = \begin{bmatrix} 0 & 0 & (e_{r\theta} + \bar{e}_{r\theta}\Delta T) \\ 0 & 0 & (e_{rx} + \bar{e}_{rx}\Delta T) \\ 0 & 0 & (e_{rr} + \bar{e}_{rr}\Delta T) \end{bmatrix}^T \begin{bmatrix} \varepsilon_\theta \\ \varepsilon_x \\ \varepsilon_r \end{bmatrix} + \begin{bmatrix} \varepsilon_{\theta\theta} & 0 & 0 \\ 0 & \varepsilon_{\theta\theta} & 0 \\ 0 & 0 & \varepsilon_{rr} \end{bmatrix} \begin{bmatrix} 0 \\ 0 \\ E_r \end{bmatrix} + \begin{Bmatrix} p_\theta \\ p_\theta \\ p_r \end{Bmatrix} \Delta T \tag{8}$$

where ε_{ik} are the dielectric permittivities measured at constant strain and temperature and p_i are the pyroelectric coefficients measured at constant strain. In the preceding two equations the piezoelectric stress constants, defined as $e_{i\alpha} + \bar{e}_{i\alpha}\Delta T$ (where $e_{i\alpha}$ is measured at constant temperature), are the matrix products of the stiffness matrix and the piezoelectric strain constants (typically denoted as d), or

$$e_{n\alpha} = d_{n\beta}C_{\beta\alpha} \qquad \text{and} \qquad \bar{e}_{n\alpha} = \bar{d}_{n\beta}C_{\beta\alpha} \tag{9}$$

where summation is implied on the repeated subscripts. The first subscript on the piezoelectric stress and strain coefficients denotes the direction of the electric field and the second denotes the direction of the induced stress (Greek subscripts represent reduced notation, that is, they vary from 1 to 6). The additional term $\bar{e}_{i\alpha}$ does not normally appear in conventional piezoelectric relations nor is it included in current analytical formulations. This term, however, represents the strong coupling between the piezoelectric stress coefficient and temperature as derived using a thermodynamic approach.[22,24]

With a little forethought it is obvious that the only pertinent electric displacement quantity is

$$D_r = (e_{r\theta} + \bar{e}_{r\theta}\Delta T)\varepsilon_\theta + (e_{rx} + \bar{e}_{rx}\Delta T)\varepsilon_x + (e_{rr} + \bar{e}_{rr}\Delta T)\varepsilon_r + \varepsilon_{rr}E_r + p_r\Delta T \tag{10}$$

The equilibrium equations for this problem, neglecting body forces, reduce to

$$\frac{1}{r}\frac{\partial(r\sigma_{rr})}{\partial r} - \frac{\sigma_{\theta\theta}}{r} = 0 \tag{11}$$

The governing equation for the electric displacement is

$$\frac{\partial D_r}{\partial r} + \frac{D_r}{r} = 0 \tag{12}$$

Solution to the differential equation (12) is

$$D_r = C_1/r \tag{13}$$

where C_1 is an arbitrary constant determined from boundary conditions. Using Eq. (13) in Eq. (10) and solving for the electric field we obtain

$$E_r = (1/\varepsilon_{rr})[(C_1/r) - (e_{r\theta} + \bar{e}_{r\theta}\Delta T)\varepsilon_\theta - (e_{rx} + \bar{e}_{rx}\Delta T)\varepsilon_x - (e_{rr} + \bar{e}_{rr}\Delta T)\varepsilon_r - p_r\Delta T] \tag{14}$$

Substituting Eq. (14) into Eq. (8), our modified constitutive relations become

$$\begin{Bmatrix} \sigma_\theta \\ \sigma_x \\ \sigma_r \end{Bmatrix} = \begin{bmatrix} \bar{C}_{\theta\theta} & \bar{C}_{\theta x} & \bar{C}_{\theta x} \\ \bar{C}_{x\theta} & \bar{C}_{xx} & \bar{C}_{xr} \\ \bar{C}_{r\theta} & \bar{C}_{rx} & \bar{C}_{rr} \end{bmatrix} \begin{Bmatrix} \varepsilon_\theta \\ \varepsilon_x \\ \varepsilon_r \end{Bmatrix} - \left(\begin{bmatrix} C_{\theta\theta} & C_{\theta x} & C_{\theta x} \\ C_{x\theta} & C_{xx} & C_{xr} \\ C_{r\theta} & C_{rx} & C_{rr} \end{bmatrix} \times \begin{Bmatrix} \alpha_\theta \\ \alpha_x \\ \alpha_r \end{Bmatrix} + \begin{bmatrix} 0 & 0 & (e_{r\theta} + \bar{e}_{r\theta}\Delta T) \\ 0 & 0 & (e_{rx} + \bar{e}_{rx}\Delta T) \\ 0 & 0 & (e_{rr} + \bar{e}_{rr}\Delta T) \end{bmatrix} \begin{Bmatrix} 0 \\ 0 \\ p_r \end{Bmatrix} \right) \Delta T - \begin{bmatrix} 0 & 0 & (e_{r\theta} + \bar{e}_{r\theta}\Delta T) \\ 0 & 0 & (e_{rx} + \bar{e}_{rx}\Delta T) \\ 0 & 0 & (e_{rr} + \bar{e}_{rr}\Delta T) \end{bmatrix} \begin{Bmatrix} 0 \\ 0 \\ C_1/r\varepsilon_{rr} \end{Bmatrix} \tag{15}$$

Equation (15) describes the response of an electrothermoelastic system. The overbar stiffness matrix is defined as

$$\begin{aligned}
\bar{C}_{\theta\theta} &= C_{\theta\theta} + \frac{(e_{r\theta} + \bar{e}_{r\theta}\Delta T)^2}{\varepsilon_{rr}} \\
\bar{C}_{\theta x} &= C_{\theta x} + \frac{(e_{r\theta} + \bar{e}_{r\theta}\Delta T)(e_{rx} + \bar{e}_{rx}\Delta T)}{\varepsilon_{rr}} \\
\bar{C}_{xx} &= C_{xx} + \frac{(e_{rx} + \bar{e}_{rx}\Delta T)^2}{\varepsilon_{rr}} \\
\bar{C}_{\theta r} &= C_{\theta r} + \frac{(e_{r\theta} + \bar{e}_{r\theta}\Delta T)(e_{rr} + \bar{e}_{rr}\Delta T)}{\varepsilon_{rr}} \\
\bar{C}_{rr} &= C_{rr} + \frac{(e_{rr} + \bar{e}_{rr}\Delta T)^2}{\varepsilon_{rr}} \\
\bar{C}_{xr} &= C_{xr} + \frac{(e_{rx} + \bar{e}_{rx}\Delta T)(e_{rr} + \bar{e}_{rr}\Delta T)}{\varepsilon_{rr}}
\end{aligned} \tag{16}$$

These new stiffness coefficients represent the relationship between stiffness measured at constant electric field to those measured under constant electric displacement conditions. Equations (16) indicate that the material stiffness measured under constant dielectric displacement conditions is temperature dependent. This dependence is physically related to changes in the depolarizing field represented by the temperature-dependent piezoelectric strain coefficients. Stiffness coefficients measured under constant electric field conditions are independent of depolarizing field effects and, thus, independent of temperature. This statement assumes that the basic crystal structure is not strongly influenced by temperature, e.g., does not undergo a phase transition. Using the constitutive relations in Eq. (15) and the equilibrium equation (11) with strain displacement relations (6), the reduced set of governing equations is found to be

$$\begin{aligned}
\bar{C}_{rr}\left[\frac{\partial^2 u_r}{\partial r^2} + \frac{1}{r}\frac{\partial u_r}{\partial r}\right] - \bar{C}_{\theta\theta}\frac{u_r}{r^2} &= \frac{\varepsilon_x}{r}(\bar{C}_{\theta x} - \bar{C}_{rx}) + \frac{\Delta T}{r} \\
\times\left[\begin{array}{l}(C_{\theta r} - C_{\theta\theta})\alpha_\theta + (C_{rx} - C_{\theta x})\alpha_x + (C_{rr} - C_{\theta r})\alpha_r \\ \quad + [(e_{r\theta} + \bar{e}_{r\theta}\Delta T) - (e_{rr} + \bar{e}_{rr}\Delta T)]p_r\end{array}\right] \\
- \frac{C_1}{r^2\varepsilon_{rr}}(e_{r\theta} + \bar{e}_{r\theta}\Delta T)
\end{aligned} \tag{17}$$

The solution to this second-order differential equation is

$$u_r = A_1 r^{n_1} + A_2 r^{n_2} + (h_1\varepsilon_{xx} + h_2\Delta T)r + h_3(C_1/\varepsilon_{rr}) \tag{18}$$

where

$$n_{1,2} = \pm\sqrt{\bar{C}_{\theta\theta}/\bar{C}_{rr}} \tag{19}$$

and

$$\begin{aligned}
h_1 &= \frac{(\bar{C}_{x\theta} - \bar{C}_{rx})}{(\bar{C}_{rr} - \bar{C}_{\theta\theta})} \\
h_2 &= \frac{(C_{r\theta} - C_{\theta\theta})\alpha_\theta + (C_{rx} - C_{\theta x})\alpha_x + (C_{rr} - C_{\theta r})\alpha_r + [(e_{r\theta} + \bar{e}_{r\theta}\Delta T) - (e_{rr} + \bar{e}_{rr}\Delta T)]p_r}{\bar{C}_{rr} - \bar{C}_{\theta\theta}} \\
h_3 &= \frac{(e_{r\theta} + \bar{e}_{r\theta}\Delta T)}{\bar{C}_{\theta\theta}}
\end{aligned} \tag{20}$$

Using Eqs. (18), (6), (14), and (5) the electric potential becomes

$$\begin{aligned}
\phi = -\frac{C_1}{\varepsilon_{rr}}\ell_n r + \frac{(e_{r\theta} + \bar{e}_{r\theta}\Delta T)}{\varepsilon_{rr}}\left[A_1\frac{r^n}{n} - A_2\frac{r^{-n}}{n} + (h_1\varepsilon_x\right. \\
\left. + h_2\Delta T)r + h_3\frac{c_1}{\varepsilon_{rr}}\ell_n r\right] + \frac{(e_{rx} + \bar{e}_{rx}\Delta T)}{\varepsilon_{rr}}\varepsilon_x r + \frac{(e_{rr} + \bar{e}_{rr}\Delta T)}{\varepsilon_{rr}} \\
\times\left[A_1 r^n + A_2 r^{-n} + (h_1\varepsilon_x + h_2\Delta T)r\right] + \frac{p_r}{\varepsilon_{rr}}\Delta T r + C_2
\end{aligned} \tag{21}$$

The radial and circumferential strain can be found using Eq. (6) and the electric field can be calculated using Eq. (5). The stresses for this problem can then be calculated from Eq. (15). The constants (A_1, A_2, C_1, C_2) in Eq. (21) are found by applying boundary conditions.

Solution for N-Cylinder System

The solution methodology for a set of concentric cylinder system comprising N materials is presented. The unknown coefficients for each material region are A_1^i, A_2^i, C_1^i, and C_2^i (where $i = 1, N$). The problem thus posed consists of $4N$ unknowns. The radii, the coordinate axes, and the displacements are defined in Fig. 1 for an N-material system. Boundary conditions to solve this problem are either mechanical displacements or tractions and either electric potentials or radial electric displacements. In this presentation, we use mechanical displacements and electrical potentials as the boundary conditions, with other approaches easily implemented. The radial displacement at the outside radius is either known or found from

$$u_r^N(r_N) = u_r^{\text{appl}} = r_N\varepsilon_r^{\text{appl}} \tag{22}$$

where the effective radial strain $\varepsilon_r^{\text{appl}}$ is known or can be calculated from effective medium concepts.[28] The effective axial strain $\varepsilon_x^{\text{appl}}$ defined in Eq. (6) is also known or can be calculated from similar effective medium concepts. The electric potential along the outer boundary and the innermost material, assuming that the inner material is conductive, is

$$\phi^2(r_1) = v_1^{\text{appl}} \qquad \phi^N(r_N) = v_N^{\text{appl}} \tag{23}$$

The first potential boundary condition is applied to material 2 at $r = r_1$ where the electrode is placed for this specific case. Continuity conditions at the material interfaces (where $i = 1, N-1$) are

$$\begin{aligned}
u_r^i(r_i) &= u_r^{i+1}(r_i), & \sigma_r^i(r_i) &= \sigma_r^{i+1}(r_i) \\
\phi^i(r_i) &= \phi^{i+1}(r_i), & D_r^i(r_i) &= D_r^{i+1}(r_i)
\end{aligned} \tag{24}$$

These equations and the fact that stresses are finite at the origin provide a framework to calculate all $4N$ coefficients using standard matrix solution techniques.

Power Requirements

An analytical model is presented to predict the power required to operate a piezoelectric material. A staircase style voltage (see insert in Fig. 8) is assumed because it provides high-fidelity control for a system.[12] Power requirements for control hardware have not been included in these calculations and the derivation presented assumes that the material is mechanically free to deform. The following model is an adaptation of the equations used to evaluate power consumption in a dielectric with power defined as the voltage times current for an electric circuit. The power dissipated in a dielectric per time period T is

$$\bar{P} = \frac{1}{T}\int_0^T IU\,dt \tag{25}$$

where I is the current and U is the applied voltage. Moulson and Herbert[27] did this calculation for piezoelectric materials using a

sinusoidal voltage input of frequency ω and arrived at the following:

$$\bar{P} = \tfrac{1}{2} E_0^2 \omega V \varepsilon_0 \varepsilon_r \tan\delta \tag{26}$$

where δ is the phase lag for a capacitor, ε_0 the permittivity of free space, ε_r the relative permittivity, $\varepsilon_r \tan\delta$ the dielectric loss factor, V is volume of the dielectric, and E_0 the amplitude of applied sinusoidal electric field.

A staircase voltage can be approximated as a ramp function for the analysis if the discrete steps are assumed to be small relative to the amplitude of the peak voltage. The ramp input voltage is written as a function of time t, with U_0 being the maximum voltage and ω being the frequency of the applied voltage, in the following Fourier series:

$$U = U_0 \left[\frac{1}{2} - \frac{4}{\pi^2} \left(\cos(\omega t) + \frac{\cos(3\omega t)}{3^2} + \frac{\cos(5\omega t)}{5^2} + \cdots \right) \right] \tag{27}$$

The current is the derivative of the charge Q on the capacitor that is found by solving the differential equation for an LRC (inductor, resistor, capacitor) circuit,

$$L\frac{\partial^2 Q}{\partial t^2} + R\frac{\partial Q}{\partial t} + \frac{1}{C}Q = U \tag{28}$$

Using Eq. (27) in Eq. (28) and solving for the charge and then differentiating gives the current in series form:

$$I = \omega U_0 C \frac{4}{\pi^2} \left[\sin(\omega t - \psi_1) + \frac{\sin(3\omega t - \psi_3)}{3} + \frac{\sin(5\omega t - \psi_5)}{5} + \cdots \right] \tag{29}$$

where ψ_i is the phase angle by which the current I lags the voltage U. The average power dissipated is found by using Eqs. (27) and (29) in Eq. (25):

$$\bar{P} = \frac{16 U_0^2 \omega C}{\pi^4} \left[\sin(\psi_1) + \frac{\sin(\psi_3)}{3^2} + \frac{\sin(\psi_5)}{5^2} + \cdots \right] \tag{30}$$

Since the phase lag δ is a small angle for ceramic piezoelectric materials, $\sin\delta \approx \tan\delta$. Therefore, for small frequency ratios, ψ_i can be related to δ by

$$\begin{aligned} \tan\psi_1 &= \tan\delta \\ \tan\psi_3 &= 3\tan\delta \\ \tan\psi_5 &= 5\tan\delta \end{aligned} \tag{31}$$

It is more common to express Eq. (30) in terms of dielectric material parameters such as the average electric field $E_0 = U_0/h$, the absolute permittivity $\varepsilon_r\varepsilon_0 = Ch/A$, and the piezoelectric volume $V = Ah$ (Ref. 27). The thickness of the material parallel to the electric field is h, and A is the area perpendicular to the electric field. The average power dissipated for our system can now be rewritten as

$$\bar{P} = \frac{16 E_0^2 \omega \varepsilon_r \varepsilon_0 V \tan(\delta)}{\pi^4} \left(1 + \frac{1}{3} + \frac{1}{5} + \cdots \right) \tag{32}$$

This is a convergent series shown by using the ratio test ($|a_{n+1}/a_n| < 1$). The percent difference between Eq. (30) with 10 terms compared to Eq. (32) is only 0.65% for PZT-5H. Therefore, we conclude that the small angle approximation is valid for the type of materials of interest here.

Results

Experimental evidence indicates that the response of piezoelectric materials are strongly dependent on temperature.[21] Therefore, when evaluating the electrothermomechanical behavior of piezoelectric materials this effect cannot be neglected. In Fig. 2 we present experimental data along with the higher-order constitutive relation used herein. The figure represents the strong dependence of the piezoelectric strain coefficients on temperature. Moderate changes in temperature (i.e., approximately 20–30 K) cause the piezoelectric coefficients to degrade 20% whereas larger temperature excursions degrade them as much as 75%. The correlation presented in the figure demonstrates the accuracy of the proposed constitutive model described in Eqs. (7) and (9) over a wide temperature range.

Table 1 Material properties for cylindrically orthotropic system used in analysis

Property\material	PZT-5H	Epoxy	Silver	Alumina
E_x, GPa	81.967	3.5	76	345
E_r, GPa	68.493	3.5	76	345
υ_{xr}	0.397	0.36	0.3	0.22
υ_{xt}	0.336	0.36	0.3	0.22
d_{31} (pC/N)	−250	0	0	0
d_{33} (pC/N)	500	0	0	0
ε_{rr} (F/m)	1.061E-8	1	1	1
CTE, $\mu\varepsilon/^\circ$C	4	30	19.6	3.01
Pyro. coeff., C/m$^2{}^\circ$C	0	0	0	0
$\tan\delta$	0.087	N/A	N/A	N/A

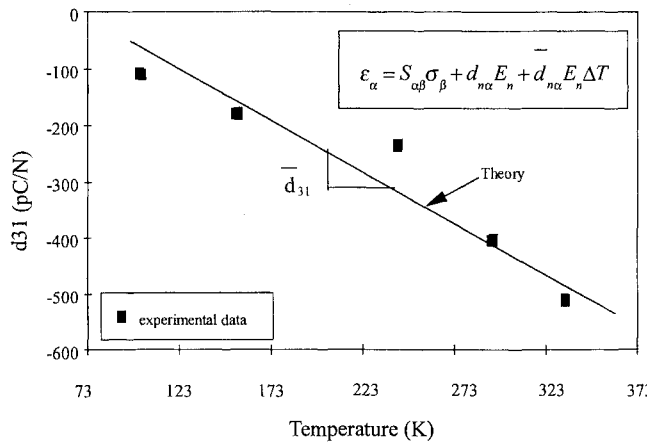

Fig. 2 Evaluation of the proposed constitutive relation incorporating the dependence of the piezoelectric strain coefficients with temperature.

In the following study, a material system constructed from four concentric cylindrical regions is analyzed. These listed (in order from the center) are alumina shaft, silver liner, epoxy, and PZT-5H (see Fig. 1). This specific system was chosen because it is representative of a linear motor used in commercial applications. The operational principle of the linear motor is a based on a sequential clamping and elongation/contraction causing translation along the shaft. Table 1 presents the electrothermomechanical properties for each of the materials studied in this paper. The pyroelectric coefficients are assumed to be negligible based on previous studies,[29] which indicate that they asymptotically approach zero as the temperature is lowered. Researchers have also shown that the pyroelectric coefficients minimally influence the electromechanical response of a piezoelectric medium.[19]

In Fig. 3 we present the stress induced in each element of the linear motor during a typical clamping sequence resulting from an applied voltage difference of 600 V at room temperature. This voltage induces a compressive interface stress of 2.92 MPa (Fig. 3) at the interface between the liner and the shaft. Assuming that the coefficient of friction between the liner and the shaft is 0.23, the static load-carrying capability for a linear motor is predicted to be 8.3 kg (i.e., approximately 83.0 N). This analytical result is the same order of magnitude reported by the manufacturer[12] (i.e., approximately 4 kg or 40 N). Differences are attributed to local eccentricities in the shaft causing the theoretical predictions to be larger than experimentally measured ones.

The clamping stress in the linear motor at room temperature as a function of the liner's thickness and Young's modulus is investigated next. Ideally, this stress should be as large as possible to maximize the clamping force onto the shaft by the piezoelectric. In Fig. 4 the clamping stress at the interface between the shaft and liner resulting

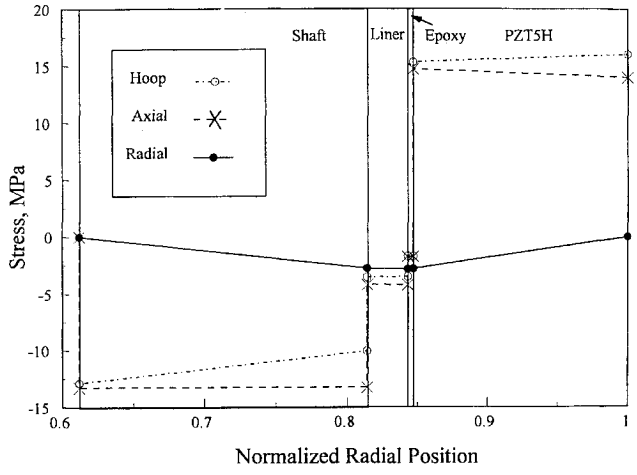

Fig. 3 Stresses in a linear motor as a function of normalized radial position with an average electric field of 0.59 MV/m.

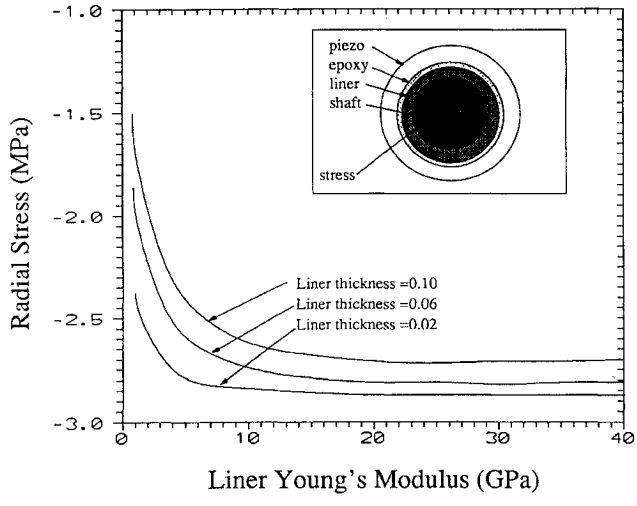

Fig. 4 Radial stress in a linear motor at the interface between the linear and the shaft with an average electric field of 0.59 MV/m; thickness and Young's modulus of the liner is varied.

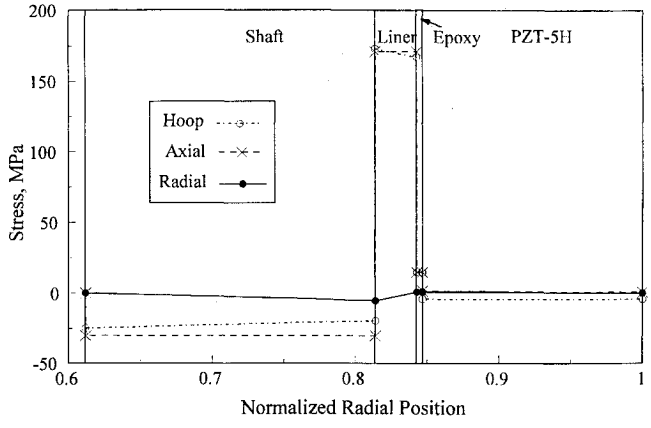

Fig. 5 Stresses in a linear motor as a function of normalized radial position with an applied $\Delta T = -100$ K.

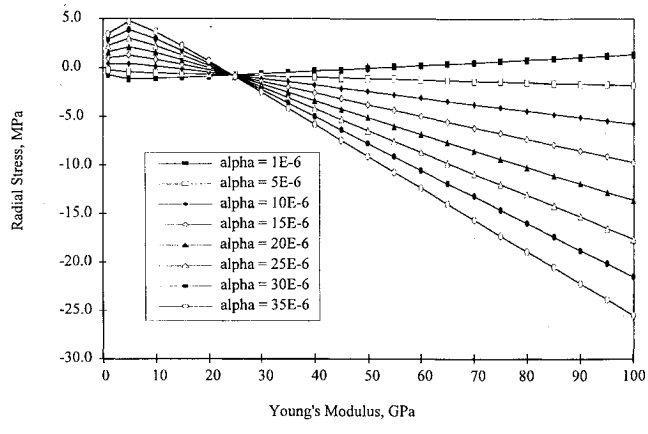

Fig. 6 Radial stress in a linear motor at the interface between the liner and the shaft for a $\Delta T = -100$ K. Young's modulus and the coefficient of thermal expansion α for the liner is varied with a liner thickness of 0.10 of total radius.

from applied Δvolts of 100 V is presented. Results demonstrate that for stiff liners (i.e., above 20 GPa) the clamping stress does not change appreciably, whereas for compliant liners (i.e., below 20 GPa), the change in clamping stress is significant. This result indicates that the Young's modulus for the liner material should be at least 20 GPa. The results presented in Fig. 4 also indicate that the stress at the shaft/liner interface changes moderately as a function of liner thickness. Therefore, for the range of liner thicknesses considered plausible for a linear motor, thickness values do not have a significant influence on the stress induced by the electric field.

The biggest problem with operation of the linear motor at reduced temperatures is the mismatch in CTEs of the various materials. In Fig. 5 we present the clamping stress generated at the interface between the liner and shaft when the temperature is decreased to 190 K. The additional clamping stress causes the linear motor to lock up and become inoperable at low temperatures as experimentally measured in our laboratories. The clamping stress presented in Fig. 5 is larger than the voltage-induced stresses presented in Fig. 3. Therefore the electromechanical response of the piezoelectric material cannot be used to alleviate the thermally induced stresses.

In Fig. 6, a parametric study is presented to evaluate the thermally induced stresses. The temperature applied to the motor is $\Delta T = -100$ K (i.e., operated at 190 K) and the liner material's stiffness and CTE values are systematically varied in the study. An interesting crossover point appears in Fig. 6, at which the clamping stress is functionally independent of the CTE values. On the left side of this point, the radial stress at the shaft/liner interface becomes larger as the CTE gets larger (for a constant Young's modulus) and is reversed on the right side of the point. Putting this in perspective, on the left side of the point a decrease in temperature causes the inner radius (refer to Fig. 1) of the liner to shrink toward the inner radius of the piezoelectric material because the liner is more compliant than the piezoelectric material. This causes the radial stress to become more positive (i.e., reduction in clamping stress) as the CTE of the liner is increased. One physical explanation for this phenomenon is that the PZT material restrains the liner from contracting onto the inner shaft. For the right side of the point, the liner material is stiffer than the piezoelectric, and the liner overcomes the restraining force imparted by the PZT material. In this latter case the liner shrinks onto the shaft and reduces the radial stress (i.e., increases the clamping stress) at the shaft/liner interface as the CTE is raised. Figure 6 also indicates that the radial stress at the shaft/liner interface will be constant for a specific value of the liner's CTE. This CTE proves to be a weighted average of the CTEs of the surrounding materials. Using Fig. 6, a material can be chosen to minimize the thermally induced clamping stresses in the linear motor.[30]

Experimental tests were conducted on the drive portion of a linear motor consisting of PZT-5H, epoxy, and a silver liner. In Fig. 7 hoop and axial strain measurements as a function of applied voltage (electric field) are presented for two temperatures ($T = 170$ and 210 K). These experimental tests indicate that the piezoelectric strain coefficients are functionally dependent on electric field strength. To evaluate this dependence, tests were performed on monolithic piezoelectric flat specimens of similar composition at room temperature, $T = 243$ K (Ref. 24). Using these data a piecewise approximation of the piezoelectric coefficients as a function of electric field was constructed[30] and used in the model. Predictions at lower temperatures were obtained by extrapolating the piecewise approximations measured at room temperature with the higher-order constitutive relation described by Fig. 2. These relations were then integrated into

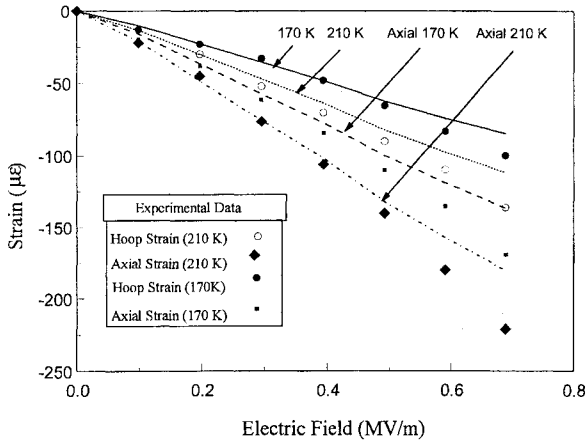

Fig. 7 Comparison between theoretical predictions and experimental results of strain vs electric field for different temperatures.

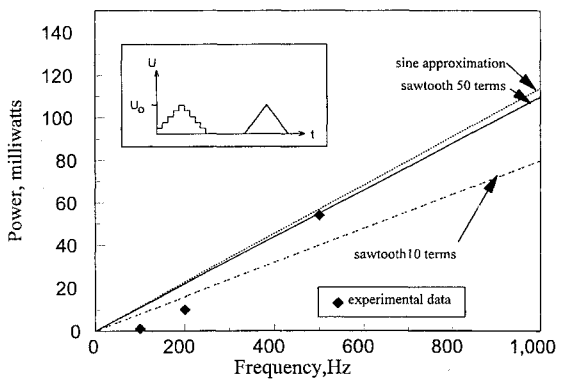

Fig. 8 Power requirement for a linear motor as a function of operational frequency.

the analytical model developed here. In Fig. 7, we present the theoretical predictions for both hoop and axial strains at $T = 170$ and 210 K using this approach. The agreement between the experimental values and the theoretical strain values in Fig. 7 are well within reason. Differences are attributed to the fact that the piezoelectric flats were obtained from a different manufacturer than the piezoelectric cylinders. Based on these results, the augmented constitutive relations provide an avenue to extrapolate nonlinear phenomena measured at room temperature to other temperature regimes.

Experimental tests were also conducted on a cylindrical piezoelectric motor to evaluate the plausibility of using the motor in deep space applications. Initial thermal tests indicated that the motor became ineffective at temperatures below 273 K. To increase the motors operating range at colder temperatures, some of the liner was removed through a honing process to reduce the thermally induced clamping stresses. The temperature was decreased to 168 K, where operation was proven feasible.[30]

In Fig. 8 we present power calculations for operating the piezoelectric ceramic at different frequencies, along with experimental data. Convergence issues were investigated by evaluating Eq. (32) with a varying number of terms. We found that 50 terms provides sufficient accuracy for this study. Comparing the power calculation developed in Eq. (32) to the simple sine wave in Eq. (26), minor differences are seen. This suggests that the sinusoidal voltage input can be used to approximate the ramp function input. Typical operating frequencies for the motor are less than 2000 Hz, suggesting that the power consumption is below 1W for this solid state motor. Experimental data obtained from Wang et al.[24] and plotted in this figure support the analytical predictions. Differences at low frequencies are due to the dependence of the loss factor on operating frequencies (see Ref. 24).

Conclusion

We presented a coupled axisymmetric electrothermal-mechanical model to represent the quasi-static response of a layered piezoelectric material system. The governing equations for the problem were derived using conventional approaches coupled with a higher-order constitutive model incorporating the thermal dependence of the piezoelectric properties. The analytical model suggests that the stiffness measured at constant electric displacement conditions is temperature dependent because of depolarizing field effects. Parametric studies on a linear motor indicate that mismatches in the thermal expansion coefficients present the biggest problem for operating the linear motor in deep space. However, the problem can be overcome by an appropriate redesign. Results obtained from experimental tests on a linear motor supported the analytical models predictions for both local strains and operational characteristics in a thermal environment. These results also suggest that the nonlinear dependence of the piezoelectric coefficients with electric field can be extrapolated to lower temperatures using the proposed constitutive relation. Power requirements for the solid state motor are in the subwatt regime if control electronics are disregarded, and we assume that appreciable mechanical loads are not supported during operation. In addition to these findings, results available in the literature indicate that radiation exposures expected in deep space will not affect the proposed electromechanical actuators.

Acknowledgments

The authors would like to extend their sincere appreciation to Burleigh Instruments, Inc., for their generous donation of linear motors to the program as well as the advice that they provided during the project. We also would like to thank the contract monitors Paul Henry and Greg Berman of the Jet Propulsion Laboratory, California Institute of Technology (Contract 959851), who provided useful insights into this problem, as well as Yoseph Bar-Cohen of the Jet Propulsion Laboratory, California Institute of Technology, whose visions helped bring about this research.

References

[1]Schubert, S., "ACTEX Flight Experiment: Development Issues and Lessons Learned," *Smart Structures and Intelligent Systems*, edited by N. Hagood and G. Knowles, *SPIE Proceedings*, Vol. 1917, 1993, pp. 510–521.

[2]Choi, K., and Chang, F. K., "Identification of Foreign Object Impact in Structures Using Distributed Sensors," *2nd International Conference on Intelligent Materials* (Williamsburg, VA), edited by C. Rogers and G. Wallace, Technomic, Lancaster, PA, 1994, pp. 361–372.

[3]Fanson J. L., Anderson, E. H., and Rapp, D., "Active Structures for Use in Precision Control of Large Optical Systems," *Optical Engineering*, Vol. 29, No. 11, 1990, pp. 1320–1327.

[4]Carman, G., Stam, M., and Wang, D., "Design of Electromechanical System for Pluto Fly-by Mission," Final Rept. for Jet Propulsion Lab., Contract 95985, Mechanical, Aerospace, and Nuclear Engineering Dept., Univ. of California, Los Angeles, CA, Jan. 1995.

[5]Niedermann, P., Emch, R., and Descouts, P., "Simple Piezoelectric Translation Device," *Review of Scientific Instruments*, Vol. 59, No. 2, 1988, pp. 368, 369.

[6]Sakuta, S., Katsunobo, U., Kiyoshi, O., Yoshinaga, M., and Sumiya, M., "Precision Dual Positioning System," *Current Developments in Optical Engineering IV*, Vol. 1334, Society of Photo-Optical Instrumentation Engineers, San Diego, CA, 1990, pp. 10–17.

[7]Kurosawa, M., and Ueha, S., "Hybrid Transducer Type Ultrasonic Motor," *IEEE Transactions on Ultrasonics, Ferroelectrics, and Frequency Control*, Vol. 38, No. 2, 1991, pp. 89–92.

[8]Kurosawa, M., Yamada, H., and Ueha, S., "Hybrid Transducer Type Ultrasonic Linear Motor," *Japanese Journal of Applied Physics*, Vol. 28, Supplement 28-1, 1988, pp. 158–160.

[9]Ohnishi, O., et al., "Piezoelectric Ultrasonic Motor Using Longitudinal-Torsional Composite Vibration of a Cylinder Resonator," *IEEE Ultrasonics Symposium* (Montreal, PQ, Canada), edited by B. R. McAvoy, Inst. of Electrical and Electronics Engineers, 1989.

[10]Kuribayashi, K., "A New Servo Motor Using Shape Memory Alloy," Inst. of Electrical and Electronics Engineers, 1989, pp. 238–243.

[11]Restorff, J. B., Teter, J. P., Vranish, J. M., and Naik, D. P., "Magnetostrictive Motor Development," *Recent Advances in Adaptive and Sensory Materials and Their Applications*, Technomic, Lancaster, PA, 1992, pp. 430–436.

[12]Anon., "UHVL Inchworm® Motor Instruction Manual," Burleigh Instruments, Inc., Fishers, NY.

[13]Newton, D., Garcia, E., and Horner, G. C., "Development of a Linear Piezoelectric Motor," *Proceedings of the Adaptive Structures Forum* (Hilton Head, SC), AIAA, Washington, DC, 1994, pp. 101–106 (AIAA Paper 94-1742).

[14]Avery, W. B., and Herakovich, C. T., "Effect of Fiber Anisotropy on Thermal Stresses in Fibrous Composites," *Journal of Applied Mechanics*, Vol. 53, Dec. 1986, pp. 751–755.

[15]Cohen, D., and Hyer, M. W., "Residual Thermal Stresses in Cross-Ply Graphite-Epoxy Tubes," *Advances in Aerospace Sciences and Engineering*, edited by U. Yuceoglu and R. Hesser, ASME Publication AD-08, American Society of Mechanical Engineers, New York, 1984, pp. 87–93.

[16]Paine, J. S. N., Rogers, C. A., and Smith, R. A., "Adaptive Composite Materials with Shape Memory Alloy Actuators for Cylinders and Pressure Vessels," *Journal of Intelligent Material Systems and Structures*, Vol. 6, No. 2, 1995, pp. 210–219.

[17]Mitchell, J. A., and Reddy, J. N., "Study of the Effect of Embedded Piezoelectric Layers in Composite Cylinders," *Smart Structures and Intelligent Systems*, edited by N. Hagood and G. Knowles, SPIE Proceedings, Albuquerque, NM, Vol. 1917, 1993, pp. 440–450.

[18]Adelman, N. T., Stavsky, Y., and Segal, E., "Axisymmetric Vibrations of Radially Polarized Piezoelectric Ceramic Cylinders," *Journal of Sound and Vibration*, Vol. 38, 1975, pp. 245–254.

[19]Tzou, H. S., and Ye, R., "Piezothermoelasticity and Control of Piezoelectric Laminates Exposed to a Steady-State Temperature Field," *Intelligent Structures, Materials, and Vibrations*, Vol. 58, Sept. 1993, pp. 27–34.

[20]Dunn, M., "Thermally Induced Fields in Electroelastic Composite Materials, Average Fields and Effective Behavior," *Journal of Engineering Materials and Technology*, Vol. 116, No. 2, 1994, pp. 200–207.

[21]Jaffe, H., and Berlincourt, D. A., "Piezoelectric Transducer Materials," *Proceedings of the IEEE*, Vol. 53, No. 11, 1965, pp. 1372–1386.

[22]Parton, V. Z., and Kudryavtsev, B. A., *Electromagnetoelasticity*, Gordon and Breach, New York, 1988, Chap. 1.

[23]Ikeda, T., *Fundamentals of Piezoelectricity*, Oxford Univ. Press, Oxford, England, UK, 1990, Chap. 2.

[24]Wang, D., Zhu, J., Huang, P., Carman, G. P., and Kim, C. J., "Evaluating the Electro-Mechanical Response of a Meso-Scale Actuator" Adaptive Structures and Material Systems Symposium (San Francisco, CA), American Society of Mechanical Engineers—WAM, 1995, Paper 95-WA/AD-7.

[25]Benedetto, J. M., Moore, R. A., Mclean, F. B., and Brody, P. S., "The Effect of Ionizing Radiation on Sol Gel Ferroelectric PZT Capacitors," *IEEE Transactions on Nuclear Science*, Vol. 37, No. 6, 1990, pp. 1713–1717.

[26]Lorenz, R. D., et al., "An Impact Penetrometer for a Landing Spacecraft," *Measurement Science and Technology*, Vol. 5, No. 9, 1994, pp. 1033–1041.

[27]Moulson, A. J., and Herbert, J. M., *Electroceramics*, Chapman and Hall, New York, 1990, Chaps. 1, 2.

[28]Pagano, N., and Tandon, G. P., "Elastic Response of Multidirectional Coated Fiber Composites," *Composite Science and Technology*, Vol. 31, 1988, pp. 273–293.

[29]Cook, W. R., Jr., Berlincourt, D. A., and Schole, F. J., "Thermal Expansion and Pyroelectricity in Lead Titanate Zirconate and Barium Titanate," *Journal of Applied Physics*, Vol. 34, No. 5, 1963, pp. 1392–1398.

[30]Stam, M., "Analysis of an Axisymmetric Piezoelectric Linear Motor Subjected to Thermal Loads," M.S. Thesis, Mechanical, Aerospace, and Nuclear Engineering Dept., Univ. of California, Los Angeles, CA, March 1995.

[31]Carman, G., Stam, M., and Wang, D., "Analytically/Experimentally Evaluating the Response of Cylindrical Piezoelectric Material Systems Subjected to Thermal Loads," *SPIE Proceedings*, Vol. 2443, 1995, pp. 434–445.